

STATISTICS

Multifractal Analysis of Soil Spatial Variability

Alexandra N. Kravchenko, Charles W. Boast, and Donald G. Bullock*

ABSTRACT

Multifractal formalism was utilized to study variability of different soil properties, including soil-test P and K, organic matter content, pH, Ca and Mg contents, and cation exchange capacity. Data from 1752 samples collected from a 259-ha agricultural field in central Illinois were used in the study. Based on the theory of multifractals a set of generalized fractal dimensions, $D(q)$, and an $f(\alpha)$ spectrum were computed for each of the studied soil properties. The $D(q)$ curves were fitted with a three-parameter mathematical function, which produced excellent fitting results with the coefficient of determination between measured and fitted values higher than 0.98 for all the studied data sets. We analyzed precision produced by the inverse distance interpolation procedure with different power to distance values and found the optimal power value to be related to one of the studied multifractal parameters. For the studied data, the multifractal parameter was the only data property that could be used as an a priori indicator of an optimal power value. The research demonstrated, first, that multifractal parameters reflected many of the major aspects of soil data variability and provided a unique quantitative characterization of the data spatial distributions and, second, that multifractal parameters might be useful for choosing an appropriate interpolation procedure for mapping soil data.

EVALUATION of soil spatial variability is an important issue in agricultural and environmental research. Fractal theory (Mandelbrot, 1982) is one of the tools that can be used to investigate and quantitatively characterize spatial variability at a large range of measurement scales (Burrough, 1993). Fractal theory has been used to study precipitation distributions (Lovejoy and Mandelbrot, 1985), geomorphological and topographical land features (Mark and Aronson, 1984; Unwin, 1989; Chase, 1992; Snow and Mayer, 1992; Turcotte, 1992), vegetation patterns (De Jong and Burrough, 1995), and crop variability (Eghball et al., 1997), as well as soil properties (Burrough, 1983a, 1983b; Armstrong, 1986; Culling, 1986; Culling and Datko, 1987; Eghball et al., 1993).

Most fractal theory applications in soil science use a monofractal approach, which assumes that soil spatial distribution can be uniquely characterized by a single fractal dimension. However, monofractal distributions "are unlikely to occur in landscapes because contemporary patterns are the results of several processes that dominated in the past" (Milne, 1991) and each of the processes contributed individually to the complexity of

the modern landscape. Hence, a single fractal dimension might not always be sufficient to represent complex and heterogeneous behavior of soil spatial variations. A recently developed extension of the monofractal approach describes the data with a set of fractal dimensions (Mandelbrot, 1974), instead of a single value. This set is called a multifractal spectrum and the method of variability characterization based on the multifractal spectrum is referred to as a multifractal analysis (Frisch and Parisi, 1985).

The multifractal approach implies that a statistically self-similar measure can be represented as a combination of interwoven fractal sets with corresponding scaling exponents. A combination of all the fractal sets produces a multifractal spectrum that characterizes variability and heterogeneity of the studied variable. The advantage of the multifractal approach is that the multifractal parameters can be independent of the size of the studied objects (Cox and Wang, 1993), as well as that no assumption is required about the data following any specific distribution (Scheuring and Riedi, 1994). Potential applications of multifractal concepts include sampling designs, quantitative descriptions and comparisons of the studied properties, and determination of the processes influencing spatial distributions, among others (Pascual et al., 1995).

The multifractal approach has been used to characterize variability of many natural phenomena, including spatial distributions of rainfall (Olsson and Niemczynowicz, 1996), characteristics of mineral deposits (Cheng et al., 1994; Agterberg, 1995) and surface fractures (Agterberg et al., 1996), spatial distributions of earthquake epicenters and landslides (Geilikman et al., 1990; Godano et al., 1996; Goltz, 1996), analysis of vegetation patterns (Scheuring and Riedi, 1994), and zooplankton biomass (Pascual et al., 1995), among others. However, very little further information exists about the multifractality of soils and soil properties. Folorunso et al. (1994) used multifractal theory for analyzing spatial distribution of soil surface strength and found multifractal parameters to be superior to a single fractal dimension in distinguishing between soil types. Muller (1996) used multifractal analysis to characterize pore space in chalk and noticed that multifractal properties are closely related to chalk permeability and porosity.

One of the reasons to characterize soil spatial variability is to select an appropriate interpolation method for development of soil property distribution maps. One method extensively used in agricultural applications is the inverse distance weighting interpolation technique.

A.N. Kravchenko and D.G. Bullock, Dep. of Crop Sciences, and C.W. Boast, Dep. of Natural Resources and Environmental Sciences, 1102 S. Goodwin Ave., Univ. of Illinois, Urbana, IL 61801. Received 29 Sept. 1998. *Corresponding author (dbullock@uiuc.edu).

This method estimates values at unsampled locations based on the measurements from the surrounding sites, with certain weights assigned to each of the measurements. It has been shown that the inverse distance parameters (e.g., a search radius, a number of closest neighboring points used for the estimation, and a power to distance value used for calculating the weights) can significantly affect the interpolation quality (Isaaks and Srivastava, 1989; Weber and Englund, 1994; Gotway et al., 1996). It is apparent that the parameters are related to the spatial variability patterns of the studied property. However, literature provides rather inconclusive and controversial information regarding statistical or geostatistical data characteristics that could serve as a priori indicators for optimal values of the inverse distance parameters (Weber and Englund, 1994; Gotway et al., 1996; Kravchenko and Bullock, 1999).

In this study, we used multifractal analysis to investigate the variability of soil P and K, organic matter content, pH, Ca, Mg, and cation exchange capacity (CEC) data. Our first objective was to determine whether the soil properties exhibit multifractal features in their spatial distributions and whether multifractal parameters could be used to describe and compare variability of different soil properties. The second objective was to evaluate possibilities of using multifractal information to determine the optimal parameters of the inverse distance interpolation technique for soil data mapping.

MATERIALS AND METHODS

Data

We used soil test P and K, organic matter content (OM), pH, Ca, Mg, and CEC data collected from a 259-ha agricultural

field in central Illinois. The field has been on a corn–soybean rotation for at least 20 years and has been managed as two contiguous equally sized fields for the entire time. A total of 1752 samples were collected from the studied field on a semiregular grid with the distance between sampling locations varying from 2 m to 50 m. Sampling locations are shown in Fig. 1a.

Multifractal Analysis

Since detailed information about multifractal procedures can be found elsewhere (Evertsz and Mandelbrot, 1992; Feder, 1988; Baveye and Boast, 1998), we review the methods used in the study (Agterberg, 1995) only briefly. First, a set of different grids with square cells of the size δ was superimposed on the studied field. Each grid cell was characterized by a grid size, δ , and a soil property value in the cell, μ_i . Five grid sizes were considered in the study, 50, 100, 200, 400, and 800 m, with the total number of cells in each grid being 1024, 256, 64, 16, and 4, respectively (Fig. 1). The minimum grid size was chosen so that every initial cell contained at least one sample (Fig. 1a). The soil property value in each of the initial cells, μ_{ini} , was set equal to the sample measurement if the cell contained only one sample, or to the average of the sample measurements if there was more than one sample in the cell. For each of the six cells with missing samples (farmhouse location), μ_{ini} was set equal to the measurement from the nearest sample. The μ_i values in the cells of the other grid sizes were calculated based on the μ_{ini} values as shown in Fig. 1 (a–e). For every grid cell of the size δ , we calculated a probability mass function, $\mu_i(\delta)$, by

$$\mu_i(\delta) = \mu_i / \mu^* \tag{1}$$

where μ^* is calculated as a sum of μ_{ini} from all the initial cells contained in the field. The distribution of the probability mass function was then analyzed for multifractality using the method of moments (Evertsz and Mandelbrot, 1992). A partition function, $\chi_q(\delta)$, of order q was calculated from the $\mu_i(\delta)$ values as

$$\chi_q(\delta) = \sum_{i=1}^n \mu_i^q(\delta) \tag{2}$$

where n is the total number of the cells of the size δ , and q is a real number ranging from $-\infty$ to ∞ . For multifractally distributed measures, the partition function scales with the cell size as

$$\chi_q(\delta) \propto \delta^{\tau(q)} \tag{3}$$

where $\tau(q)$ is the mass exponent of order q . The mass exponent for each q -value can be obtained by plotting $\log \chi_q(\delta)$ vs. $\log \delta$. For $q \geq 1$, the value of $\chi_q(\delta)$ is largely determined by the large data values, while the influence of the small data values increases with decreasing q . For $q \leq -1$, the small-value data contribute most to the $\chi_q(\delta)$. Thus, the multifractal approach, in effect, separates the data into subsets dominated by high or low data values, and quantifies the fractal properties of these subsets. If the probability function $\mu_i(\delta)$ in the neighborhood of the cell scales with the cell size as $\mu_i(\delta) \propto \delta^\alpha$, then, for $\delta \rightarrow 0$, the singularity exponent α is a scaling property peculiar to the cell. Parameter α is also called a local fractal dimension or a singularity index. The local fractal dimension can be determined by Legendre transformation of the $\tau(q)$ curve (Evertsz and Mandelbrot, 1992) as

$$\alpha(q) = d\tau(q)/dq \tag{4}$$

The number of cells of size δ with the same α , $N_\alpha(\delta)$, is related to the cell size as $N_\alpha(\delta) \propto \delta^{-f(\alpha)}$, where $f(\alpha)$ is a scaling exponent of the cells with common α . Parameter $f(\alpha)$ can be calculated as

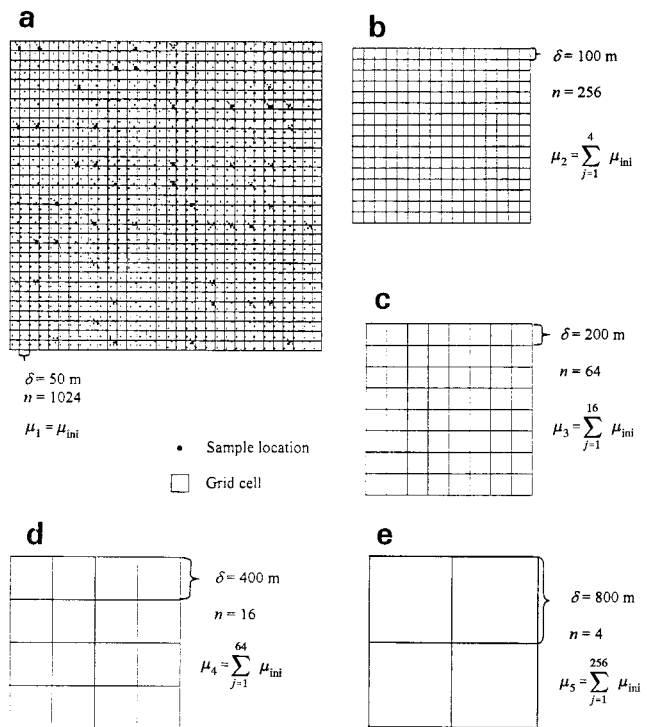


Fig. 1. Sample locations and five grids used in the multifractal calculations, with grid sizes ranging from (a) 50 m to (e) 800 m. For each grid, we show the grid size, δ , the total number of the cells in the grid, n , and the equation for calculating soil property value in the grid cell, μ_i , based on the soil property values in the initial cells, μ_{ini} .

$$f[\alpha(q)] = q\alpha(q) - \tau(q) \tag{5}$$

A plot of $f(\alpha)$ vs. α is called a multifractal spectrum. For $\mu_s(\delta)$ monofractally distributed through the studied area, α remains the same for all the cells of the same size and the multifractal spectrum consists of a single point. In the case of a multifractal distribution, the spectrum has a concave downward curvature, with a range of α -values increasing correspondingly to the increase in the distribution's heterogeneity.

The $f(\alpha)$ spectrum is related to the other commonly used set of multifractal exponents known as generalized fractal dimensions (Hentschel and Procaccia, 1983), calculated from the mass exponent function as

$$D(q) = \tau(q)/(q - 1) \tag{6}$$

The fractal dimension at $q = 0$, $D(0)$, equals the box-counting dimension of the geometric support of the measure being studied—which is, in our case, the Euclidean dimension of a plane (i.e., 2). The information fractal dimension, $D(1)$, is obtained at $q = 1$ using l'Hôpital's rule, and the correlation fractal dimension, $D(2)$, is obtained at $q = 2$.

Inverse Distance Weighting

Inverse distance weighting estimates the value of variable Z at unsampled location x_0 , $Z^*(x_0)$, based on the data from m surrounding locations, $Z(x_i)$, as (Isaaks and Srivastava, 1989)

$$Z^*(x_0) = \sum_{i=1}^m w_i Z(x_i) \tag{7}$$

where w_i are the weights assigned to each $Z(x_i)$ value and m is the number of closest neighboring sampled data points used for the estimation. The weights for inverse distance are defined as (Isaaks and Srivastava, 1989)

$$w_i = \frac{1/d_i^p}{\sum_{i=1}^m 1/d_i^p} \tag{8}$$

where d_i is the distance between the point being estimated and the sampled point, and p is an exponent parameter. Exponent values of 2, 3, and 4 are the most commonly used in agricultural applications. In this study, we compared the inverse distance interpolations with p -values from 1 to 4 in increments of 0.2, and with the number of closest neighboring points used for the estimation ranging from 5 to 30. The search radius was chosen so that it was large enough to include the required number of the closest points. To define the optimal p -value and the optimal number of closest neighbors, we eliminated in turn each value from the data set and used the inverse distance weighting to estimate the value based on the information from the rest of the data. Estimation criteria were the mean squared error (MSE)

$$MSE = 1/m \sum_{i=1}^m \{[Z^*(x_i) - Z(x_i)]^2\} \tag{9}$$

and the mean absolute error (MAE)

$$MAE = 1/m \sum_{i=1}^m [|Z^*(x_i) - Z(x_i)|] \tag{10}$$

RESULTS AND DISCUSSION

Variability of the soil properties was evaluated using statistical and geostatistical analyses. For the statistical analysis, we calculated coefficients of variation (CV), skewness, kurtosis, and positive and negative maximum relative deviations from the sample mean obtained as $[Z(x_i) - Z_m]/Z_m$, where $Z(x_i)$ is the soil property value at location x_i and Z_m is the sample mean. A statistical summary of the studied data is presented in Table 1.

For the geostatistical analysis, sample semivariograms were computed using the geostatistical software package GSLIB (Deutsch and Journel, 1998). To ensure comparable semivariogram results, data values were standardized prior to sample semivariogram calculation as $[Z(x_i) - Z_m]/\sigma$, where σ is the standard deviation. Sample semivariograms were fitted with spherical variogram models and adequacy of the chosen models was tested using cross-validation (Deutsch and Journel, 1998). Cross-validation criteria used for the model parameter selection were the correlation coefficient between measured and estimated values, mean absolute error (Myers, 1991), and the reduced kriging variance (Zhang et al., 1992). Variogram model parameters, such as nugget and range, are presented in Table 1.

For each of the studied soil properties, we calculated the $f(\alpha)$ multifractal spectrum (Eq. [4] and [5]) with q ranging from -15 to 15 in increments of 0.2 . Plots of the partition function $\chi_q(\delta)$ vs. cell size δ in a log-log scale for P, Mg, pH, and CEC are shown in Fig. 2a, 2b, 2c, and 2d, respectively. All of the log-transformed $\chi_q(\delta)$ plots were straight lines for $-15 < q < 15$, signifying that the studied soil properties can be regarded as multifractal measures (Evertsz and Mandelbrot, 1992). The coefficient of determination (r^2) for fitting log-transformed $\chi_q(\delta)$ plots with straight lines was larger than 0.99 for all the studied data. Selected multifractal parameters, such as minimum and maximum values of α and $f(\alpha)$, information fractal dimension, $D(1)$, and correlation fractal dimension, $D(2)$, are shown in Table 1. The minimum values of α and $f(\alpha)$, α_{\min} and $f(\alpha_{\min})$, corre-

Table 1. Statistical, geostatistical, and multifractal characteristics of the studied soil properties along with the optimal values of the power to distance (p) and the number of closest neighbors (m) used for the data interpolation with the inverse distance procedure.

| Soil property† | Mean | CV | Skewness | Kurtosis | Nugget | Range | Multifractal parameters‡ | | | | | | | |
|----------------|------|----|----------|----------|--------|-------|--------------------------|--------|-----------------|-----------------|--------------------|--------------------|-----|-----|
| | | | | | | | $D(1)$ | $D(2)$ | α_{\min} | α_{\max} | $f(\alpha_{\min})$ | $f(\alpha_{\max})$ | p | m |
| P | 59.1 | 70 | 2.64 | 8.70 | 0.080 | 395 | 1.951 | 1.884 | 1.329 | 2.441 | -0.092 | -0.152 | 1.4 | 5 |
| K | 375 | 45 | 4.71 | 32.27 | 0.108 | 218 | 1.983 | 1.951 | 1.341 | 2.127 | -0.740 | 1.270 | 2.6 | 15 |
| Ca | 4654 | 20 | 1.30 | 4.25 | 0.202 | 61 | 1.995 | 1.990 | 1.858 | 2.114 | 1.018 | 1.237 | 2.6 | 19 |
| Mg | 657 | 24 | 1.47 | 0.24 | 0.138 | 137 | 1.993 | 1.985 | 1.754 | 2.109 | 0.511 | 1.369 | 3.0 | 15 |
| pH | 6.37 | 7 | 0.56 | 0.55 | 0.270 | 243 | 2.000 | 1.999 | 1.980 | 2.013 | 1.835 | 1.913 | 1.6 | 15 |
| OM | 3.19 | 11 | -0.54 | 0.11 | 0.293 | 146 | 1.999 | 1.998 | 1.976 | 2.051 | 1.847 | 1.624 | 0.8 | 5 |
| CEC | 17.1 | 16 | 1.22 | 2.87 | 0.166 | 152 | 1.996 | 1.992 | 1.819 | 2.056 | 0.535 | 1.702 | 2.6 | 14 |

† OM, organic matter; CEC, cation exchange capacity.

‡ Multifractal parameters: $D(1)$, information fractal dimension; $D(2)$, correlation fractal dimension; $\alpha_{\min} = \alpha$ at $q = 15$; $f(\alpha_{\min}) = f(\alpha)$ at $q = 15$; $\alpha_{\max} = \alpha$ at $q = -15$; $f(\alpha_{\max}) = f(\alpha)$ at $q = -15$.

spond to q of 15, while the maximum values, α_{\max} and $f(\alpha_{\max})$, correspond to q of -15 . Only one set of grid sizes was considered in the study. Hence, only one unique multifractal spectrum was obtained for each soil property. Folorunso et al. (1994) observed variations in shapes of multifractal spectra of soil surface strength data collected at different sampling scales. Further analysis is necessary to examine the influence of sampling scale and grid size on the shape of the multifractal spectra.

Generalized fractal dimensions $D(q)$ (Eq. [6]) were calculated on the range of q -values from 0 to 15. Experimental $D(q)$ curves were fitted with a mathematical function as

$$D(q) = a/[1 + (bq)^c]^{1-1/c} \quad [11]$$

where a , b , and c are empirical parameters (van Genuchten, 1980). Fitting was conducted using a nonlinear least-squares optimization procedure that minimized the sum of squared errors between experimental and fitted $D(q)$ values (Kool et al., 1987). Except for the K data, Eq. [11] produced an excellent description of $D(q)$ curves, with coefficients of determination (r^2) higher than or equal to 0.996. Experimental and fitted $D(q)$ curves with corresponding coefficients of determination are presented in Fig. 3a for P, Ca, Mg, and OM and in Fig. 3b for K, pH, and CEC.

Multifractal spectra were found to be comprehensive characteristics of all the major aspects of the data variability. Correlation coefficients (r) between soil statistical and multifractal properties significant at the 0.05 significance level are shown in Table 2. Significant corre-

lations were observed between the data coefficients of variation and the majority of the multifractal parameters. Appearance of the extremely high and extremely low data values were related to the left ($q \geq 1$) and right ($q \leq -1$) parts of the $f(\alpha)$ spectrum, respectively. The maximum negative deviation from the mean, Z_- , was significantly correlated with α_{\max} and $f(\alpha_{\max})$. The maximum positive deviation, Z_+ was correlated with α_{\min} and $f(\alpha_{\min})$ values (Table 2). Both skewness and kurtosis were correlated with α_{\min} , whereas skewness was also correlated with $f(\alpha_{\min})$. Significant correlations were found between the geostatistical parameters and multifractal spectra. Both the width of the $f(\alpha)/\alpha$ spectrum and the left part of the spectrum characterized by α_{\min} and $f(\alpha)_{\min}$ were closely related to the nugget values. Parameters of the right side of the spectrum, α_{\max} and $f(\alpha)_{\max}$, were significantly correlated with range (Table 2).

To analyze the potential of multifractal spectra for describing the data spatial variability, we compared two scenarios of CEC distribution in the studied field. The first scenario corresponded to the observed distribution of CEC measurements. For the second scenario, 40 of the CEC data points were relocated in the field. For relocation, we randomly selected 40 data points out of CEC data set and then exchanged the data between the randomly selected points and 40 data points with the highest CEC values. Statistical properties of the data set remained intact and only spatial structure of the data distribution was modified. The CEC maps are shown in Fig. 4a and 4b for the first and the second scenarios, respectively. The maps were obtained using the inverse

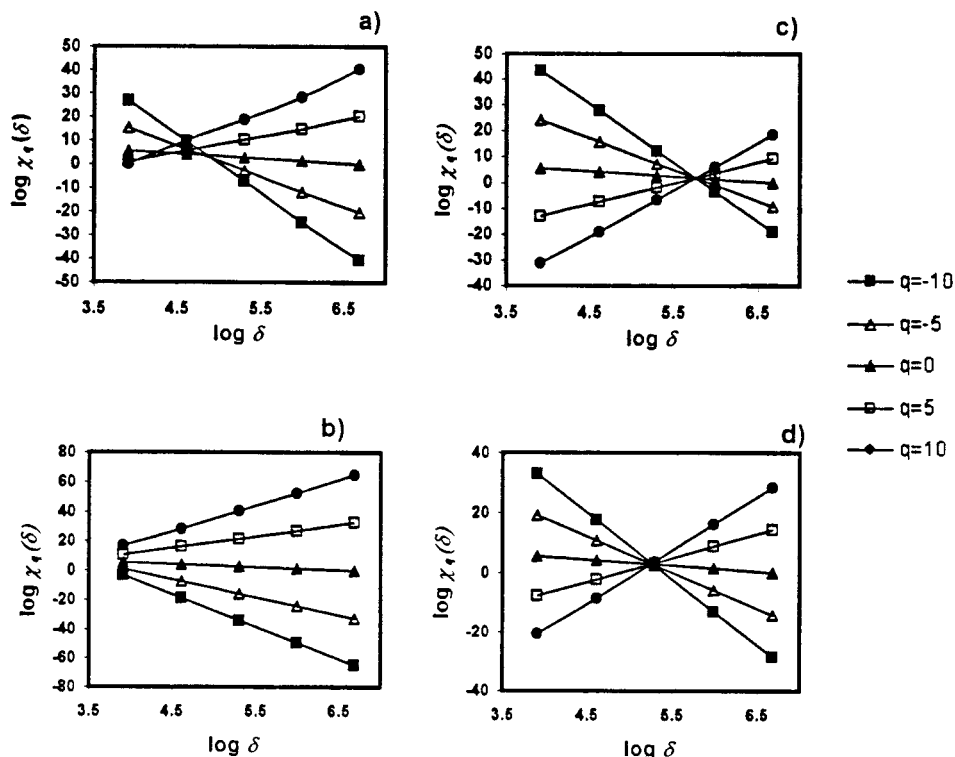


Fig. 2. Partition function $\chi_q(\delta)$ plotted vs. cell size δ in a log-log scale at selected q -values for (a) P, (b) Mg, (c) pH, and (d) cation exchange capacity (CEC). The slope of the $\log \chi_q(\delta)/\log \delta$ line defines the mass exponent $\tau(q)$ (Eq. [3]).

distance weighting with a power to distance value of 2 and the number of the closest samples of 12. Visual analysis of CEC distributions from the two scenarios revealed a number of differences (Fig. 4a and 4b). However, the differences were very little if at all reflected in corresponding sample variograms (Fig. 4c), although the multifractal spectra of the two scenarios were remarkably unlike (Fig. 4d). Comparing with the multifractal spectrum of the second scenario, the spectrum of the first scenario had an asymmetrically long left part. The left part of the spectrum describes distribution of large data values, and the symmetrical multifractal spectrum of the second scenario reflected more homogeneous distribution of the high CEC values. Multiple data points with high CEC clustered together in the first scenario caused the partitioning function (Eq. [2]) for $q \gg 1$ at small grid sizes to be larger than the partitioning function for the second scenario. At large grid sizes, the partitioning functions of both scenarios were practically the same, since the differences caused by relocation were smoothed out. Hence, values of $\tau(q \gg 1)$ for the first scenario obtained as slopes of log-log plots of partitioning functions vs. grid sizes (Eq. [3]) were lower than those for the second scenario. The differences in distribution of high CEC values were further reflected in lower α -values (Eq. [4]), and lower $f(\alpha)$ (Eq. [5]) for the left part of the first scenario. The studied example demonstrated that, comparing with the sample variogram, multifractal spectrum worked as a better characteristic of the data spatial variability. Indeed, variograms use only two first statistical moments of the variable, while multifractal approach uses a wide range of statistical moments, providing a much deeper insight into data variability structure. Comparison of the two scenarios showed that multifractal approach might be particularly effective for analyzing spatial distributions of extremely large or small data values, which is consistent with findings of Agterberg (1995), who applied multifractal analysis for characterizing giant and supergiant metal deposits.

Multifractal spectra are shown in Fig. 5 for P, K, OM, pH, Ca, Mg, and CEC. To demonstrate the relationships between the multifractal spectra and spatial features of the data distributions, we plotted corresponding soil property distribution maps. Inverse distance weighting with a power to distance value of 2 and the number of the closest samples of 12 was used to make the maps.

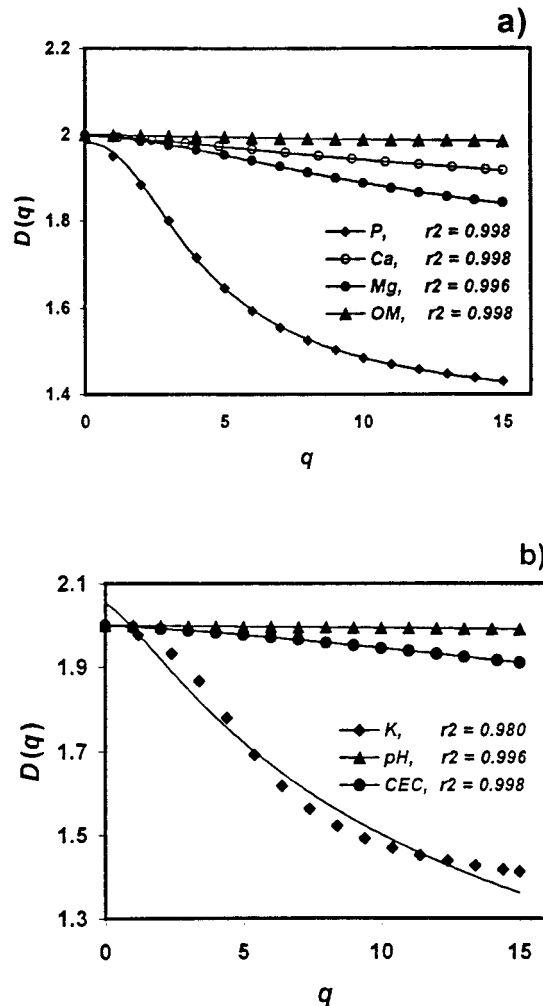


Fig. 3. Experimental $D(q)$ data and fitting curves of Eq. [11] for (a) P, Ca, Mg, and organic matter (OM) and for (b) K, pH, and cation exchange capacity (CEC).

The map classes were obtained by dividing the range of the soil property values into 12 equal-sized intervals. The width of the multifractal spectrum was related to the overall variability expressed through coefficient of variation. The shape and the degree of asymmetry of the multifractal spectrum reflected the asymmetry in the property distribution, dominance of either low or high data, as well as presence of the extremely high or extremely low data points.

Table 2. Significant ($P \leq 0.05$) correlation coefficients (r) between statistical and geostatistical soil properties and multifractal parameters.

| | Multifractal parameters‡ | | | | | | Parameters of Eq. [11] | | | | |
|---------------|--------------------------|----------------|-------------------------------|-------------------|-------------------|-------------------------------------|------------------------|--------|-------|-------|-----|
| | α_{min} | α_{max} | $\alpha_{max} - \alpha_{min}$ | $f(\alpha_{min})$ | $f(\alpha_{max})$ | $f(\alpha_{max}) - f(\alpha_{min})$ | $D(1)$ | $D(2)$ | a | b | c |
| CV | -0.935 | 0.929 | 0.993 | -0.823 | -0.925 | NS | -0.965 | -0.978 | 0.890 | 0.957 | NS |
| Skewness | -0.912 | NS | 0.806 | -0.881 | NS | NS | NS | NS | 0.871 | NS | NS |
| Kurtosis | -0.803 | NS | NS | NS | NS | NS | NS | NS | 0.836 | NS | NS |
| Z_+^\dagger | -0.969 | NS | NS | -0.892 | NS | NS | NS | NS | NS | NS | NS |
| Z_-^\dagger | NS | 0.894 | NS | NS | -0.904 | NS | NS | NS | NS | NS | NS |
| Nugget | 0.886 | NS | -0.880 | 0.980 | NS | NS | NS | 0.759 | NS | NS | NS |
| Range | NS | 0.823 | NS | NS | -0.782 | NS | -0.881 | -0.879 | NS | 0.865 | NS |

† CV, coefficient of variation; Z_+ and Z_- , positive and negative maximum relative deviations from the sample mean obtained as $(Z(x_i) - Z_m)/Z_m$, where $Z(x_i)$ is the soil property value at location x_i and Z_m is the sample mean.

‡ Multifractal parameters: $D(1)$, information fractal dimension; $D(2)$, correlation fractal dimension; $\alpha_{min} = \alpha$ at q of 15; $f(\alpha_{min}) = f(\alpha)$ at q of 15; $\alpha_{max} = \alpha$ at q of -15; $f(\alpha_{max}) = f(\alpha)$ at q of -15.

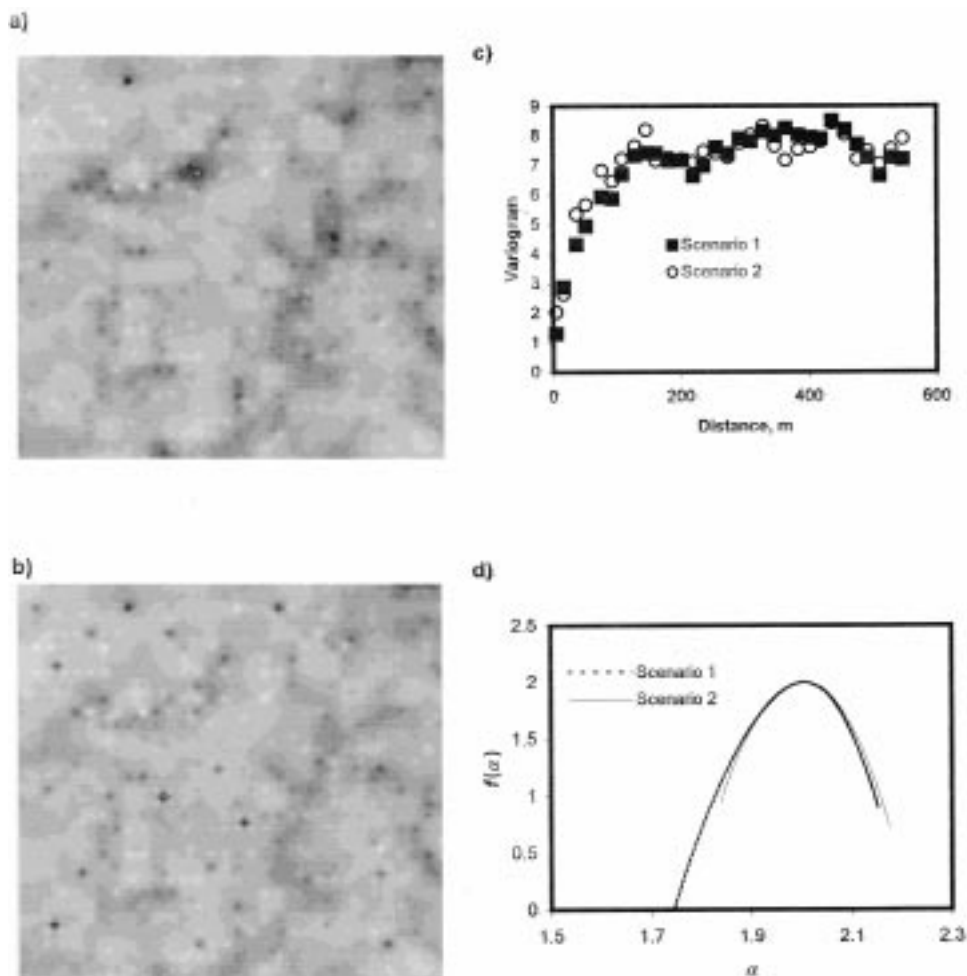


Fig. 4. Geostatistical and multifractal characteristics of the two scenarios for cation exchange capacity (CEC) data distribution. Maps of CEC data for (a) first and (b) second scenarios were obtained using inverse distance weighting and are shown, along with (c) corresponding sample variograms, and (d) multifractal spectra.

Comparison of Ca, Mg, and CEC data can be used as an example of how the spectrum reflects the spatial variability features. Although spatial distributions of Ca and CEC are relatively similar, the lower values (map classes 1 to 3) occupy a larger area on the Ca map, while higher values (map classes >4) prevail on the CEC map (Fig. 5e and 5g). Hence, the CEC multifractal spectrum displays pronounced asymmetry, comparing with the Ca spectrum. The overall variability of the two soil properties is approximately the same, which is reflected in the comparable widths of the multifractal spectra (equal to 0.237 and 0.257 for CEC and Ca, respectively). Calcium and Mg have very similar maps of low values (map classes 1 to 3), and as a result they have practically identical right parts of multifractal spectra (Fig. 5e and 5f). However, noticeable differences exist in distributions of high values (map classes >4). Areas with high data values in the Mg map contributed to a wider multifractal spectrum with an asymmetrically long left part.

For each of the studied soil properties, we performed an inverse distance interpolation with p -values ranging from 1 to 4 in increments of 0.2 and the number of closest neighbors from 5 to 30. The best values of p and m were chosen based on the MSE and MAE values and

are shown in Table 1. The priority was given to the MSE as a measure of the error distribution spread. The MAE was used afterwards to verify that selected parameters do not produce significantly biased estimations. After selecting the best power value and the optimal number of closest neighbors, we analyzed the relationships between them and statistical, geostatistical, and multifractal parameters of the studied data. Table 3 presents the correlation coefficients between soil properties and the parameters of the inverse distance interpolation. For the studied data set, the highest correlation between the soil data characteristics and the inverse distance parameters was the correlation between the best p -value and the difference between minimum and maximum $f(\alpha)$ values, $f(\alpha_{\max}) - f(\alpha_{\min})$. A plot of the optimal p -values vs. $f(\alpha_{\max}) - f(\alpha_{\min})$ is shown in Fig. 6. As can be seen from the plot, the most accurate interpolation for the data sets with negative $f(\alpha_{\max}) - f(\alpha_{\min})$ was obtained by using the p -value close to 1. Data sets with $f(\alpha_{\max}) - f(\alpha_{\min})$ in a range from 0 to 0.5 were the best interpolated with the power value of about 2, and p close to 3 produced the most accurate results for the data sets with $f(\alpha_{\max}) - f(\alpha_{\min})$ larger than 0.5. For the studied soil data sets, $f(\alpha_{\max}) - f(\alpha_{\min})$ was the only satisfactory indicator

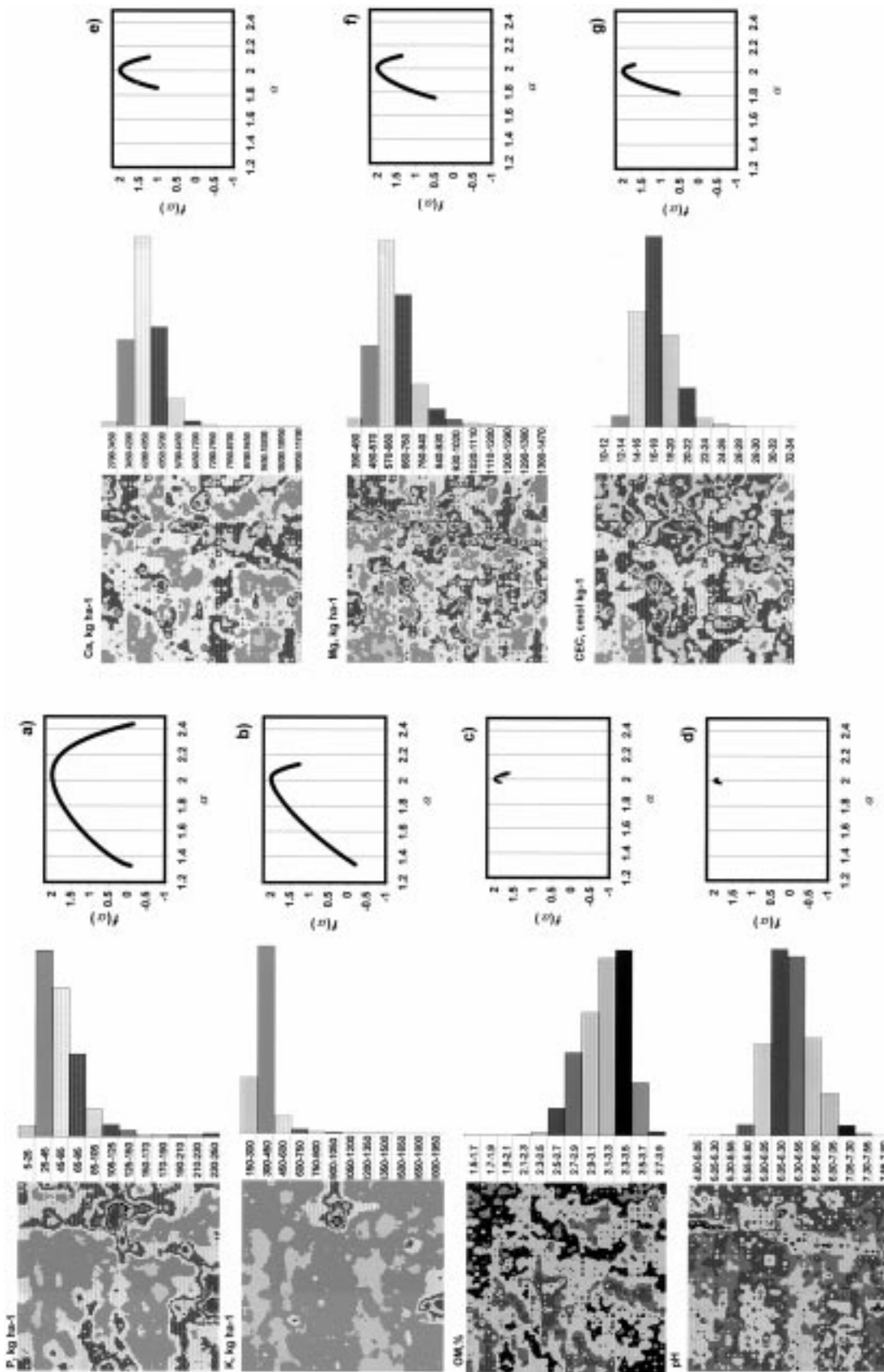


Fig. 5. Multifractional $f(\alpha)$ spectra along with soil property distribution maps and histograms for (a) P; (b) K; (c) organic matter, OM; (d) pH; (e) Ca; (f) Mg; and (g) cation exchange capacity, CEC. Maps were obtained by interpolating the experimental data using the inverse distance weighted interpolation procedure. Histogram classes correspond to map classes and were obtained by dividing the data range into 12 equal-sized intervals.

Table 3. Correlation coefficients between the inverse distance interpolation parameters, such as optimal value of the power to distance (p) and the number of closest neighbors used for the estimation (m), and selected statistical, geostatistical, and multifractal parameters of the soil data sets.

| | Coefficient of variation | Skewness | Kurtosis | Nugget | Range | $f(\alpha_{\max}) - f(\alpha_{\min})$ |
|-----|--------------------------|----------|----------|--------|--------|---------------------------------------|
| p | -0.018 | 0.451 | 0.304 | -0.489 | -0.440 | 0.715† |
| m | -0.381 | 0.195 | 0.142 | -0.013 | -0.587 | 0.472 |

† Significant at the 0.1 probability level.

of the optimal power value for the inverse distance interpolation. No significant correlation was observed between the optimal number of closest neighboring points and any of the other statistical, geostatistical, and multifractal soil parameters.

SUMMARY

The multifractal concepts were applied to analyze variability of the soil properties. Multifractal analysis revealed that all of the studied soil properties can be regarded as multifractal measures and can be characterized using the multifractal approach. Multifractal spectra of the studied data carried a large amount of spatial information and allowed quantitative differentiation between the soil variability patterns. Multifractal analysis was found to be an efficient tool for characterization, analysis, and comparison of the soil spatial variabilities. Significant correlations were found between multifractal parameters and the statistical attributes of the studied soil properties, such as coefficient of variation, skewness, and kurtosis, as well as semivariogram parameters, such as nugget and range. Since multifractal spectra provided quantitative characteristics of the differences in distributions, multifractal analysis could be used as an indicator of the appropriate interpolation technique for mapping soil data. The best power to distance of the inverse distance weighting was significantly positively correlated with the difference between the maximum and minimum $f(\alpha)$. This relationship might be used for choosing the best power value for the inverse distance estimation procedure; however, additional analysis with a larger number of variables would be desirable to verify the significance of the observed correlation. No signifi-

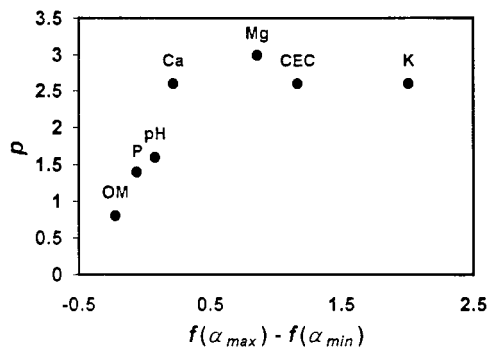


Fig. 6. The optimal values of the power to distance (p) parameter of the inverse distance interpolation procedure plotted vs. the difference between the minimum and maximum values of the multifractal parameter $f(\alpha)$, [$f(\alpha_{\max}) - f(\alpha_{\min})$].

cant correlation was found between any other statistical and geostatistical parameters of the studied soil properties and the inverse distance parameters. A three-parameter mathematical equation was successfully adopted to fit the curve of generalized fractal dimensions $D(q)$ and produced a quantitative description for the experimental set.

REFERENCES

- Agterberg, F.P. 1995. Multifractal modeling of the sizes and grades of giant and supergiant deposits. *Int. Geol. Rev.* 37:1–8.
- Agterberg, F.P., Q. Cheng, A. Brown, and D. Good. 1996. Multifractal modeling of fractures in the Lac Du Bonnet batholith, Manitoba. *Comput. Geosci.* 22:497–507.
- Armstrong, A.C. 1986. On the fractal dimension of some transient soil properties. *J. Soil Sci.* 37:641–652.
- Baveye, P., and C.W. Boast. 1998. Fractal geometry, fragmentation processes and the physics of scale-invariance: An introduction. p. 1–54. *In* P. Baveye et al. (ed.) *Fractals in soil science*. CRC Press, New York.
- Burrough, P.A. 1983a. Multiscale sources of spatial variation in soil: I. The application of fractal concepts to nested levels of soil variation. *J. Soil Sci.* 34:577–597.
- Burrough, P.A. 1983b. Multiscale sources of spatial variation in soil: II. A non-Brownian fractal model and its application in soil. *J. Soil Sci.* 34:599–620.
- Burrough, P.A. 1993. Soil variability: A late 20th century view. *Soils Fert.* 56:529–562.
- Chase, C.G. 1992. Fluvial land sculpting and the fractal dimension of topography. *Geomorphology* 5:39–57.
- Cheng, Q., F.P. Agterberg, and S.B. Ballantyne. 1994. The separation of geochemical anomalies from background by fractal models. *J. Geochem. Explor.* 51:109–130.
- Cox, L.B., and J.S.Y. Wang. 1993. Fractal surfaces: Measurement and applications in earth sciences. *Fractals* 1:87–117.
- Culling, W.E.H. 1986. Highly erratic spatial variability of soil pH on Iping Common, West Sussex. *Catena* 13:81–98.
- Culling, W.E.H., and M. Datko. 1987. The fractal geometry of the soil-covered landscape. *Earth Surf. Processes Landforms* 12:369–385.
- De Jong, S.M., and P.A. Burrough. 1995. A fractal approach to the classification of Mediterranean vegetation types in remotely sensed images. *Photogramm. Eng. Remote Sens.* 61:1041–1053.
- Deutsch, C.V., and A.G. Journel. 1998. Geostatistical software library and user's guide. Oxford Univ. Press, New York.
- Eghball, B., L.N. Mielke, G.A. Calvo, and W.W. Wilhelm. 1993. Fractal description of soil fragmentation for various tillage methods and crop sequences. *Soil Sci. Soc. Am. J.* 57:1337–1341.
- Eghball, B., R.B. Ferguson, G.E. Varvel, G.W. Hergert, and C.A. Gotway. 1997. Fractal characterization of spatial and temporal variability in site-specific and long-term studies. p. 339–348. *In* M.M. Novak and T.G. Dewey (ed.) *Fractal frontiers*. World Scientific, Singapore.
- Evertsz, C.J.G., and B.B. Mandelbrot. 1992. Multifractal measures (Appendix B). p. 922–953. *In* H.-O. Peitgen et al. (ed.) *Chaos and fractals*. Springer-Verlag, New York.
- Feder, J. 1988. *Fractals*. Plenum Press, New York.
- Frisch, U., and G. Parisi. 1985. On the singularity structure of fully developed turbulence. p. 84–88. *In* M. Gil et al. (ed.) *Turbulence and predictability in geophysical fluid dynamics*. North Holland Publ. Co., Amsterdam.
- Folorunso, O.A., C.E. Puente, D.E. Rolston, and J.E. Pinzon. 1994. Statistical and fractal evaluation of the spatial characteristics of soil surface strength. *Soil Sci. Soc. Am. J.* 58:284–294.
- Geilikman, M.B., T.V. Golubeva, and V.F. Pisarenko. 1990. Multifractal patterns of seismicity. *Earth Planet. Sci. Lett.* 99:127–132.
- Godano, C., M.L. Alonzo, and A. Bottari. 1996. Multifractal analysis of the spatial distribution of earthquakes in southern Italy. *Geophys. J. Int.* 125:901–911.
- Goltz, C. 1996. Multifractal and entropic properties of landslides in Japan. *Geol. Rundsch.* 85:71–84.
- Gotway, C.A., R.B. Ferguson, G.W. Hergert, and T.A. Peterson. 1996.

- Comparison of kriging and inverse-distance methods for mapping soil parameters. *Soil Sci. Soc. Am. J.* 60:1237–1247.
- Hentschel, H.G.R., and I. Procaccia. 1983. The infinite number of generalized dimensions of fractals and strange attractors. *Physica D* 8:435–444.
- Isaaks, E.H., and R.M. Srivastava. 1989. *An introduction to applied geostatistics*. Oxford Univ. Press, New York.
- Kool, J.B., J.C. Parker, and M.Th. van Genuchten. 1987. Parameter estimation for unsaturated flow and transport models: A review. *J. Hydrol.* 91:255–293.
- Kravchenko, A., and D.G. Bullock. 1999. A comparative study of interpolation methods for mapping soil properties. *Agron. J.* 91:393–400.
- Lovejoy, S., and B. Mandelbrot. 1985. Fractal properties of rain and a fractal model. *Tellus* 37A:209–232.
- Mandelbrot, B.B. 1974. Intermittent turbulence in self-similar cascades: Divergence of high moments and dimension of the carrier. *J. Fluid Mech.* 62:331–358.
- Mandelbrot, B.B. 1982. *The fractal geometry of nature*. W.H. Freeman, San Francisco, CA.
- Mark, D.M., and P.B. Aronson. 1984. Scale-dependent fractal dimensions of topographic surfaces: An empirical investigation, with applications in geomorphology and computer mapping. *Math. Geol.* 16:671–683.
- Milne, B.T. 1991. Lessons from applying fractal models to landscape patterns. p. 200–235. *In* M.G. Turner and R.H. Gardner (ed.) *Quantitative methods in landscape ecology*. Springer-Verlag, Berlin.
- Muller, J. 1996. Characterization of pore space in chalk by multifractal analysis. *J. Hydrol.* 187:215–222.
- Myers, D.E. 1991. Interpolation and estimation with spatially located data. *Chemomet. Intell. Lab. Syst.* 11:209–228.
- Olsson, J., and J. Niemczynowicz. 1996. Multifractal analysis of daily spatial distributions. *J. Hydrol.* 187:29–43.
- Pascual, M., F.A. Ascoti, and H. Caswell. 1995. Intermittency in the plankton: A multifractal analysis of zooplankton biomass variability. *J. Plankton Res.* 17:1209–1232.
- Scheuring, I., and R.H. Riedi. 1994. Application of multifractals to the analysis of vegetation pattern. *J. Veg. Sci.* 5:489–496.
- Snow, R.S., and L. Mayer (ed.) 1992. *Fractals in geomorphology*. *Geomorphology* 5:194–212.
- Turcotte, D.L. 1992. *Fractals and chaos in geology and geophysics*. Cambridge Univ. Press, Cambridge.
- Unwin, D. 1989. Fractals and the geosciences: Introduction. *Comput. Geosci.* 15:163–165.
- van Genuchten, M.Th. 1980. A closed-form equation for predicting the hydraulic conductivity of unsaturated soils. *Soil Sci. Soc. Am. J.* 44:892–898.
- Weber, D.D., and E.J. Englund. 1994. Evaluation and comparison of spatial interpolators: II. *Math. Geol.* 26:589–603.
- Zhang, R., D.E. Myers, and A.W. Warrick. 1992. Estimation of the spatial distribution of soil chemicals using pseudo-cross-variograms. *Soil Sci. Soc. Am. J.* 56:1444–1452.